VOLUME 19, N° 2 2025
Journal of Automation, Mobile Robotics and Intelligent Systems

A Novel Model-free Control Technique for Angular Motion of a Single Ducted-fan Unmanned Aerial Vehicle

Submitted: 26th February 2024; accepted: 9th May 2024

Thien Minh Tran

DOI: 10.14313/jamris-2025-012

Abstract:
This paper reveals the proposed method to operate the landing angular motion of a ducted-fan unmanned aerial vehicle (DUAV). The angular motion frequently varies during the landing stage. Additionally, the DUAV system is a complex system with uncertain parameters or incorrectly identified parameters, and the yaw angle has to be controlled in the proper position before grounding. Because of issues with the structure of the system and identification in the real model of DUAV, a model-free control technique is approached by combining time-delay estimation (TDE) and integral sliding mode law (ISMC). The TDE technique provides a model-free method for the complex system as DUAV. Hence, a novel control method is designed to achieve the desired angular motion. In addition, the ISMC method is a good solution for tracking performance. The stability of the whole system is guaranteed by the Lyapunov theory. We conduct a comparison between the TDE-ISMC and sliding mode control (SMC) in several cases to verify the effectiveness of the proposed TDE-ISMC control.

Keywords: *time-delay estimation, TDE, ISMC, DUAV, model-free, motion control*

1. Introduction

In recent years, there have been several notable studies of unmanned aerial vehicle systems (UAVs). Nevertheless, the single ducted-fan unmanned aerial vehicle (DUAV) is the perfect intersection of the properties of UAVs, helicopters, and missiles [1]. The DUAV belongs to the conception of UAVs, while the main power system is similar to that of a helicopter, and its motion analysis has to be considered a missile. Therefore, the configuration of DUAV is a complex system with a variety of devices such as ducted-fan [2], hover [3], aerodynamics [4, 5], and so forth. In modern aerial space technology, the mission it involves surveillance, reconnaissance, exploration, communication, and so forth in both military and civil. One other advantage of DUAV is that it can be considered successful in departing and landing from unprepared sites and small deck spaces.

Based on the characteristic operation, the stage of DUAV usually involves pre-takeoff, takeoff, flying, and landing, with landing being most important to recall the DUAV. Angular motion control, in particular, is a key in the landing process of the single DUAV.

Sometimes, the accurate dynamic model of the system is impossible to identify and estimate [6]. However, several modern control algorithms enforce correct physical parameters to obtain high tracking performance, such as super-twisting sliding mode control [7], sliding mode control [8–10], feedback control [11], pole placement control [12], adaptive control [13–15], artificial intelligence [16], etc.

It is worth noting that the motion controllability of a single ducted-fan unmanned aerial vehicle cannot be easily carried out because of the complex system and incorrectly identified physical parameters. Due to the landing process, which can lead to the instability of the whole system, the motion of the yaw angle of DUAV plays an important role during this stage as seen in Fig. 1. Before the landing process, the yaw angle needs to be controlled in the right-angle position, which establishes the stable stage for the whole DUAV. In the desired position, the professionals can foresee unexpected features during the landing process. Nevertheless, the control motion of the angle of the DUAV system before landing had received little attention.

Based on the facts mentioned above, this study proposes a new approach by a combination of time delay estimation technique and integral sliding mode control (TDE-ISMC) to tackle the complex system with incorrectly identified parameters. The TDE technique provides a model-free approach method for the complex DUAV system, while the ISMC shows a high tracking performance to dramatic fluctuations of DUAV.

Additionally, the TDE technique can estimate and compensate for the control signal, which is caused by the disadvantage of ISMC as an incorrectly identified parameter model, and the stability of the whole system is bounded by the Lyapunov theory. Furthermore, the proposed control law TDE-ISMC is compared to the classical sliding mode control in several cases to verify the feasibility and transparency. The classical SMC also has similar characteristics to ISMC so that the effectiveness of the proposed method is even more outstanding.

This paper is organized as follows. Section 2 reveals the configuration of the DUAV in yaw motion. Section 3 illustrates the control design of the proposed method TDE-ISMC, and the stability is addressed in detail, compared to the classical SMC. Numerical simulation results of the performance are presented in Section 4. Finally, Section 5 concludes the paper.

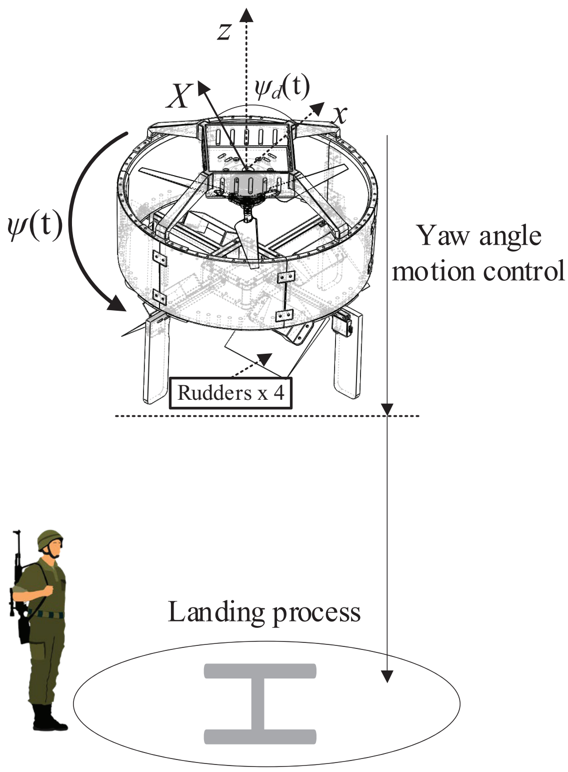

Figure 1. The yaw motion control concept of the single ducted-fan UAV

2. Configuration of the Single Ducted-fan UAV

The mathematical modeling dynamics of the single ducted-fan UAV are identified from the real physical system by a multiple-input single-output system and can be obtained as follows [12]

$$\ddot{\boldsymbol{\psi}}_*(t) = \boldsymbol{K}\boldsymbol{\tau}(t) + \boldsymbol{Q}\dot{\boldsymbol{\psi}}_*(t) + \boldsymbol{P}\boldsymbol{\psi}_*(t) \tag{1}$$

where $\boldsymbol{\psi}_*(t) = [\psi_1(t), \psi_2(t), \psi_3(t), \psi_4(t)]^T \in R^4$ is the yaw angle vector of the system, controlled by the four rudders. $\tau(t) = [\tau_1(t), \tau_2(t), \tau_3(t), \tau_4(t)]^T \in R^4$ is the control signal of the rudders. $\mathbf{K} \in R^{4\times4}$, $\mathbf{Q} \in R^{4\times4}$ and $\mathbf{P} \in R^{4\times4}$ are defined as the constant matrices, identified from the real DUAV via MATLAB. Each yaw angle in Equation (1) is operated by one of four actuators (rudder and servo motor), associated $\boldsymbol{\psi}_*(t) = \bar{\mathbf{c}}_\psi \psi(t)$, where $\bar{\mathbf{c}}_\psi \in R^4$ is a weighting column vector. By the multiple-input single-output definition, the yaw angle of the system is the sum of the elements of $\boldsymbol{\psi}_*(t)$, with the relevant weighting coefficients that are used in the following $\psi(t)$. Let the claims be true for this research.

Assumption 1. We assume that the slipstream axis is coincident with the fan axis [4].

Assumption 2. We assume that there is no strong crosswind during the experimental identification [4].

3. Control System Designs

The aim of this research is to control the yaw angle of a single DUAV $\psi(t)$ tracks the desired path properly, which means that $e(t) = \psi_d(t) - \psi(t)$ is as little as possible, noted as $\mathbf{C}_\psi \bar{\mathbf{c}}_\psi e(t)$, where, $\mathbf{C}_\psi = diag[C_{\psi_1}, C_{\psi_1}, C_{\psi_1}, C_{\psi_1}] \in R^{4\times4}$ is a positive weighting matrix.

3.1. Time-delay Estimation and Integral Sliding Mode Technique

The modeling Equation (1) of DUAV can be rearranged as follows

$$\ddot{\boldsymbol{\psi}}_*(t) = \boldsymbol{K}\boldsymbol{\tau}(t) + \boldsymbol{\Lambda}(\dot{\boldsymbol{\psi}}_*, \boldsymbol{\psi}_*). \tag{2}$$

The sliding polynomial variable [17] can be defined to achieve a control objective as follows

$$\boldsymbol{\sigma}(t) = \mathbf{C}_\psi \bar{\mathbf{c}}_\psi \dot{e}(t) + \mathbf{K_n} \mathbf{C}_\psi \bar{\mathbf{c}}_\psi e(t) + \mathbf{K_i} \mathbf{C}_\psi \bar{\mathbf{c}}_\psi \int e(t)dt \tag{3}$$

where $\boldsymbol{\sigma}(t) = [\sigma_1(t), \sigma_2(t), \sigma_3(t), \sigma_4(t)]^T \in R^4$, $\mathbf{K_n} = diag([K_{n_1}, K_{n_2}, K_{n_3}, K_{n_4}]) \in R^{4\times4}$ and $\mathbf{K_i} = diag([K_{i_1}, K_{i_2}, K_{i_3}, K_{i_4}]) \in R^{4\times4}$ are depicted as positive gains matrices for the stability of the single ducted-fan UAV. The control law is constructed based on the sliding polynomial of the integral sliding mode as follows

$$\begin{aligned}\boldsymbol{\tau}(t) = {} & \mathbf{K}^{-1}\mathbf{C}_\psi^{-1}[\mathbf{C}_\psi \bar{\mathbf{c}}_\psi \ddot{\psi}_d(t) + \mathbf{K_n}\mathbf{C}_\psi \bar{\mathbf{c}}_\psi \dot{e}(t)] \\ & + \mathbf{K}^{-1}\mathbf{C}_\psi^{-1}[\mathbf{K_i}\mathbf{C}_\psi \bar{\mathbf{c}}_\psi e(t) + \mathbf{K}_{\boldsymbol{\sigma}} \mathrm{sign}(\boldsymbol{\sigma}(t))] \\ & - \mathbf{K}^{-1}\hat{\boldsymbol{\Lambda}}(\dot{\boldsymbol{\psi}}_*, \boldsymbol{\psi}_*)\end{aligned} \tag{4}$$

where $\hat{\boldsymbol{\Lambda}}(\dot{\boldsymbol{\psi}}_*, \boldsymbol{\psi}_*)$ is the estimated term, based on Equation (2). The signum function $\mathrm{sign}(\sigma(t))$ is defined as corresponding to the elements of the input vector, whereas $\mathrm{sgn}(\sigma(t)) = [\mathrm{sgn}(\sigma_1(t)), \mathrm{sgn}(\sigma_2(t)), \mathrm{sgn}(\sigma_3(t)), \mathrm{sgn}(\sigma_4(t))]^T \in \mathrm{R}^4$. A positive control gain matrix is denoted as $\mathbf{K}_{\boldsymbol{\sigma}} = diag([K_{\sigma_1}, K_{\sigma_2}, K_{\sigma_3}, K_{\sigma_4}]) \in R^{4\times4}$.

By time-delay estimation theory [18-20], the term $\hat{\boldsymbol{\Lambda}}(\dot{\boldsymbol{\psi}}_*, \boldsymbol{\psi}_*)$ can be estimated by delaying one unit of sampling time measurement $\boldsymbol{\Lambda}(\dot{\boldsymbol{\psi}}_*, \boldsymbol{\psi}_*)$. In other words, Equation (2) is rewritten as a mathematical time delay estimation as follows

$$\hat{\boldsymbol{\Lambda}}(t) = \boldsymbol{\Lambda}(t-L) = \ddot{\boldsymbol{\psi}}_*(t-L) - \boldsymbol{K}\boldsymbol{\tau}(t-L) \tag{5}$$

where L is a sampling period. Substituting Equation (5) into Equation (4), the control law in Equation (4) can be rearranged as follows

$$\begin{aligned}\tau(t) = {} & \underbrace{-\mathbf{K}^{-1}\ddot{\boldsymbol{\psi}}_*(t-L) + \tau(t-L)}_{\text{TDE}} \\ & \underbrace{+\mathbf{K}^{-1}\mathbf{C}_\psi^{-1}[\mathbf{C}_\psi \bar{\mathbf{c}}_\psi \ddot{\psi}_d(t) + \mathbf{K_n}\mathbf{C}_\psi \bar{\mathbf{c}}_\psi \dot{e}(t)]}_{\text{ISMC}} \\ & \underbrace{+\mathbf{K}^{-1}\mathbf{C}_\psi^{-1}[\mathbf{K_i}\mathbf{C}_\psi \bar{\mathbf{c}}_\psi e(t) + \mathbf{K}_{\boldsymbol{\sigma}} \mathrm{sign}(\sigma(t))]}_{\text{ISMC}}.\end{aligned} \tag{6}$$

The proof of stability. The Lyapunov candidate can be considered as follows

$$V(t) = \frac{1}{2}\boldsymbol{\sigma}^T(t)\boldsymbol{\sigma}(t). \tag{7}$$

Substituting the control law in Equation (6) into taking the time derivative of Equations (3) and (7), the time derivative of Lyapunov can obtain

$$\begin{aligned}\dot{V}(t) &= \boldsymbol{\sigma}(t)^T\dot{\boldsymbol{\sigma}}(t)\\ &= \boldsymbol{\sigma}(t)^T[\mathbf{C}_{\psi}\bar{\mathbf{c}}_{\psi}\ddot{\psi}_d(t) - \mathbf{C}_{\psi}K\tau(t) - \mathbf{C}_{\psi}\Lambda(t)\\ &\quad \mathbf{K_n}\mathbf{C}_{\psi}\bar{\mathbf{c}}_{\psi}\dot{e}(t) + \mathbf{K_i}\mathbf{C}_{\psi}\bar{\mathbf{c}}_{\psi}e(t)]\\ &= \boldsymbol{\sigma}(t)^T\mathbf{C}_{\psi}(\hat{\boldsymbol{\Lambda}}(t) - \Lambda(t))\\ &\quad - \boldsymbol{\sigma}(t)^T\mathbf{K}_{\sigma}\mathrm{sign}(\boldsymbol{\sigma}(t))\\ \dot{V}(t) &= \boldsymbol{\sigma}(t)^T\mathbf{C}_{\psi}[\Lambda(t-L) - \Lambda(t)]\\ &\quad - \boldsymbol{\sigma}(t)^T\mathbf{K}_{\sigma}\mathrm{sign}(\boldsymbol{\sigma}(t)) \le 0. \end{aligned} \tag{8}$$

By using the time delay estimation technique, the term of $\boldsymbol{\Lambda}(t)$ is obtained, which is approximately the term of $\boldsymbol{\Lambda}(t-L)$. Therefore, the time derivative of the Lyapunov candidate in Equation (8) is semi-negative $\dot{V}(t) \le 0$. Hence, the property of the sliding polynomial variable $\boldsymbol{\sigma}(t)$ is guaranteed to be bound, and the error of tracking performance $e(t)$ also is bounded. Based on the Lyapunov-like lemma [21], the stability of the control law in Equation (6) is ensured.

3.2. Classical Sliding Mode Control

The sliding surface variable is associated as follows

$$\mathbf{s}(t) = \mathbf{C}_{\psi}\bar{\mathbf{c}}_{\psi}\dot{e}(t) + \mathbf{K_s}\mathbf{C}_{\psi}\bar{\mathbf{c}}_{\psi}e(t) \tag{9}$$

where $\mathbf{s}(t) = [s_1(t), s_2(t), s_3(t), s_4(t)]^T \in R^4$, and $\mathbf{K_s} = diag[(K_{s_1}, K_{s_2}, K_{s_3}, K_{s_4})]^T \in R^{4\times4}$ is noted as a positive control gain matrix. The control algorithm's definition is

$$\begin{aligned}\tau(t) &= \mathbf{K}^{-1}\mathbf{C}_{\psi}^{-1}[\mathbf{C}_{\psi}\bar{\mathbf{c}}_{\psi}\ddot{\psi}_d(t) - \mathbf{C}_{\psi}\boldsymbol{\Lambda}(t)]\\ &\quad + \mathbf{K}^{-1}\mathbf{C}_{\psi}^{-1}[K_s\mathbf{C}_{\psi}\bar{\mathbf{c}}_{\psi}\dot{e}(t) + \mathbf{K}_{dot}\mathrm{sign}(\mathbf{s}(t))]\end{aligned} \tag{10}$$

where $\mathbf{K}_{dot} = diag([K_{dot_1}, K_{dot_2}, K_{dot_3}, K_{dot_4}]) \in R^{4\times4}$ is depicted as a positive gain matrix. The signum function is $\mathrm{sgn}(s(t)) = [\mathrm{sgn}(s_1(t)), \mathrm{sgn}(s_2(t)), \mathrm{sgn}(s_3(t)), \mathrm{sgn}(s_4(t))]^T \in R^4$.

The Lyapunov candidate yields

$$W(t) = \frac{1}{2}\mathbf{s}^{\mathbf{T}}(t)\mathbf{s}(t). \tag{11}$$

Substituting the control law in Equation (6) into taking the time derivative of Equations (3) and (7), the time derivative of Lyapunov can obtain

$$\begin{aligned}\dot{W}(t) &= \mathbf{s}^T(t)\mathbf{s}(t)\\ \dot{W}(t) &= \mathbf{s}^T(t)[\mathbf{C}_{\psi}\bar{\mathbf{c}}_{\psi}\ddot{\psi}_d(t) - \mathbf{C}_{\psi}\boldsymbol{K\tau}(t)\\ &\quad - \mathbf{C}_{\psi}\Lambda(t) + \mathbf{K_s}\mathbf{C}_{\psi}\bar{\mathbf{c}}_{\psi}\dot{e}(t)]\\ \dot{W}(t) &= -\mathbf{s}^{\mathbf{T}}(t)\mathbf{K}_{dot}\mathrm{sign}(s(t)) \le 0.\end{aligned} \tag{12}$$

Equation (12) is also semi-negative $\dot{W}(t) \le 0$. The sliding surface variable $s(t)$ is bounded, so the error of tracking performance $e(t)$ also is bounded. Based on the Lyapunov-like lemma [21], the stability of the control law in Equation (10) is verified.

4. Numerical Simulation

4.1. Simulation Setup

The desired tracking is established in frequency, amplitude, and the property of change to compare and verify the effectiveness of the proposed control. A comparison is done in several tracking references to ensure correctness, transparency, and practicality.

The simulation with the proposed control law in Equations (6) and (10) is carried out using the real physical parameters of a single ducted-fan UAV. The identification of parameters is implemented by using the MATLAB identification toolbox. The nominal physical parameters in Equation (1) are as follows [12]

$$\begin{aligned}\mathbf{Q} &= diag[(-0.46975, -0.46975,\\ &\quad -0.46975, -0.46975)]\\ \mathbf{P} &= diag[(-0.1905, -0.1905, -0.1905, -0.1905)]\\ \mathbf{K} &= diag[(-0.501, -0.501, -0.501, -0.501)]\end{aligned}$$

The weighting vector and matrix are noted as $\bar{\mathbf{c}}_{\psi} = [0.25, 0.25, 0.25, 0.25]^T$ and $\mathbf{C}_{\psi} = diag[(1, 1, 1, 1)]$, respectively. The initial setup value for the simulation of the single ducted-fan UAV system at $t_0 = 0$ are $\psi(t_0) = 0$, $\dot{\psi}(t_0) = 0$, and $\tau(t_0) = [0, 0, 0, 0]^T$. The sampling time is defined as 1 (ms), and the low pass filter is considered as $1/(s + 1)$.

To evaluate objectively and fairly, the root mean square error (RMSE) and the integral of time multiplied by the absolute error (ITAE) in Equation (13) are implemented to measure the tracking error of both controllers.

$$ITAE(t) = \int t|e(t)|dt \tag{13}$$

4.2. Simulation Results

The results of the proposed control law, TDE-ISMC, are compared with the classical control, SMC. To be transparent and fair, both TDE-ISMC and SMC keep unchanged control coefficients in the fourth type of tracking reference.

The control gain matrices of the proposed control law in Equation (6) are denoted as $\mathbf{K}_{\boldsymbol{\sigma}} = diag[(0.81, 0.81, 0.81, 0.81)] \in R^{4\times4}$, $\mathbf{K_i} = diag[(0.0081, 0.0081, 0.0081, 0.0081)] \in R^{4\times4}$, and $\mathbf{K_n} = diag[(0.0152, 0.0152, 0.0152, 0.0152)] \in R^{4\times4}$. Similarly, the control gain matrices of the classical SMC are defined as $\mathbf{K_s} = diag[(3.01, 3.01, 3.01, 3.01)] \in R^{4\times4}$ and $\mathbf{K}_{dot} = diag[(1.1, 1.1, 1.1, 1.1)] \in R^{4\times4}$. The simulation results of the yaw angle's reference types (a) and (b) and types (c) and (d) are shown in scenario 1 (Figs. 3–10) and scenario 2 (Figs. 11–18), respectively. The shapes of types (a)–(d) are the typical input signals of the yaw angle.

The reference types (a) and (b) are similar shapes of signal; however, type (b) sharply changes with a larger amplitude. The sine wave is configured for the reference types (c) and (d), and the differences between them are frequency and amplitude.

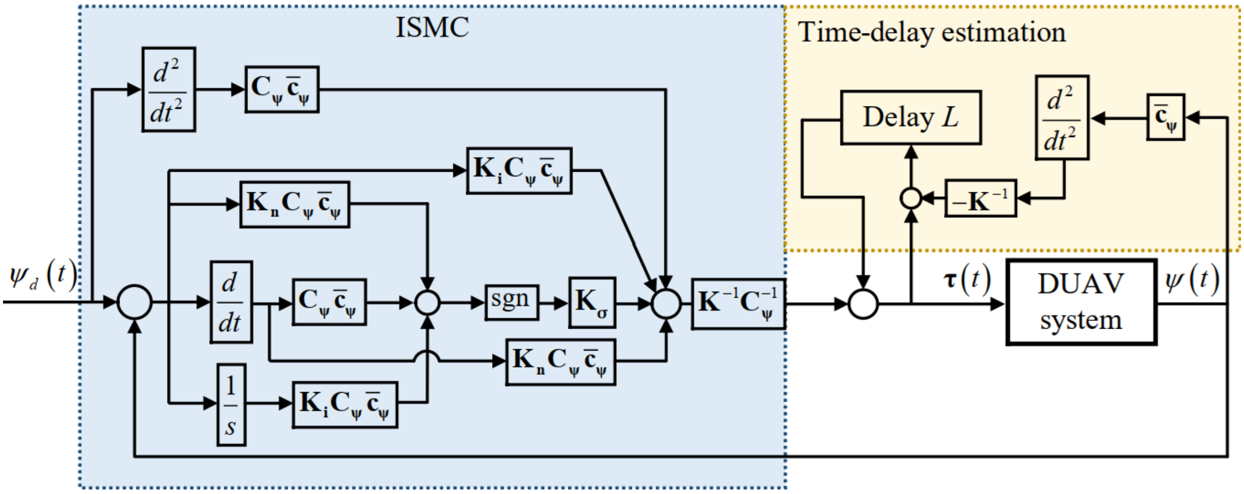

Figure 2. The proposed controller TDE-ISMC's diagram

Table 1. RMSE and ITAE in scenario #1 (trapezium waves).

Reference	RMSE		ITAE	
	Type (a)	Type (b)	Type (a)	Type (b)
TDE-ISMC	0.5223	0.5226	0.0254	0.0252
SMC	0.9967	2.5176	0.0384	0.0825

By these results, the advantages of the proposed control law are thoroughly confirmed and verified.

4.2.1. Scenario 1: Trapezium Wave

Figures 3 and 4 show the yaw angle tracking of the single ducted-fan UAV following the desired trapezium wave in detail. The proposed controller TDE-ISMC tracks closely to the reference, compared to the classical SMC. The classical SMC response is delayed a period and underdamped, which can lead the whole system to instability if the control gain matrices are not suitable. However, the proposed controller can deal with these defective terms by the properties of TDE and ISMC.

The error of the yaw angle is described in Fig. 5 (type (a)) and Fig. 6 (type (b)). The error of the classical SMC of these results varied along the curve of references and fluctuated in a larger range, compared to the proposed controller TDE-ISMC. This proves that the stability of the TDE-ISMC law is better than classical SMC. Moreover, the control signals of the proposed controller are depicted in Fig. 7 (type (a)) and Fig. 9 (type (b)), fluctuating harmonic frequency with a narrow range, compared to those of classical control law in Fig. 8 (type (a)) and Fig. 10 (type (b)). Additionally, the RMSE and ITAE values are listed in Table 1, which shows that TDE-ISMCs are better than SMCs. That thoroughly evaluates the effectiveness of the proposed control law.

4.2.2. Scenario 2: Sine wave

The sine wave of the references is established for this study simulation. There are two kinds of sine waves: type (c) and type (d). In sine wave type (d), the frequency and amplitude are larger than in type (c).

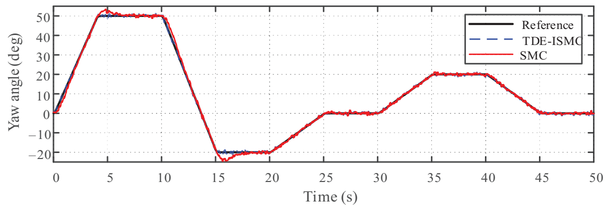

Figure 3. Tracking the performance of trapezium wave type (a) reference

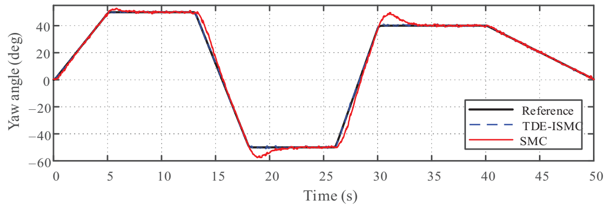

Figure 4. Tracking the performance of trapezium wave type (b) reference

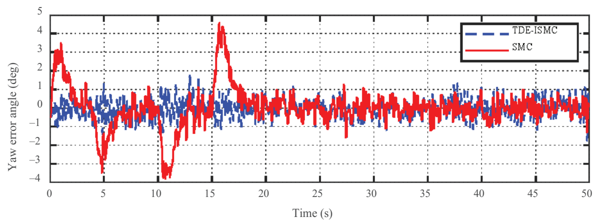

Figure 5. Error of tracking the performance of trapezium wave type (a) reference

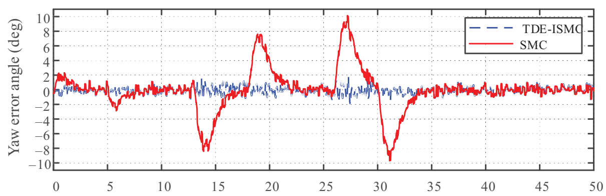

Figure 6. Error of tracking the performance of trapezium wave type (b) reference

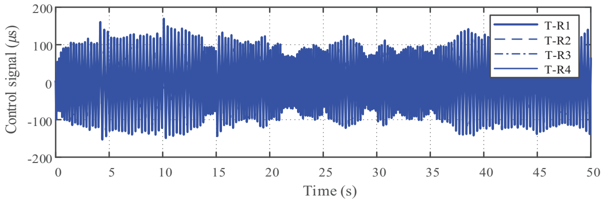

Figure 7. Control signal input of four actuators of TDE-ISMC (type a)

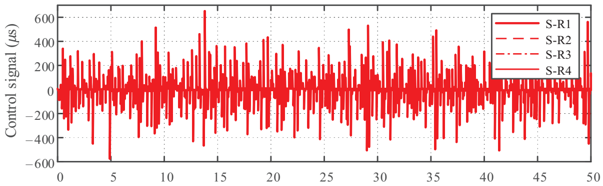

Figure 8. Control signal input of four actuators of SMC (type a)

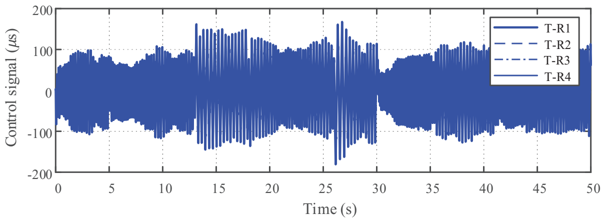

Figure 9. Control signal input of four actuators of TDE-ISMC (type b)

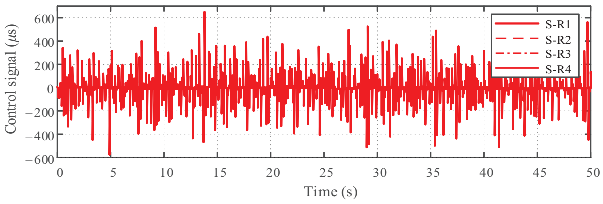

Figure 10. Control signal input of four actuators of SMC (type b)

The performance of tracking the trajectory of both references is shown in Figs. 11 and 12 in detail. In these cases of sine waves, the classical SMC behavior did not track the references in both types (c) and (d) by using similar control gain matrices as in scenario 1. Especially in type (d), the classical SMC leads the whole system to be unstable. The proposed controller TDE-ISMC tracks well in scenario 2 by using similar control gain matrices as used in scenario 1. The sine wave with large amplitude and high frequency proves the advantages of the proposed controller by using the properties of TDE and ISMC in the problem of physical systems.

Similarly, the error of the performance is illustrated in Fig. 13 (type (c)) and Fig. 14 (type (d)). In the proposed control law TDE-ISMC, the error is reduced to almost zero value after a period of response time. Hence, the stability of the whole system is guaranteed. Additionally, the control input signals are presented in Figs. 15–16 for type (c) and Figs. 17–18 for type (d).

Table 2. RMSE and ITAE in scenario #2 (sine waves).

Reference	RMSE		ITAE	
	Type (c)	Type (d)	Type (c)	Type (d)
TDE-ISMC	1.0319	4.2562	0.0465	0.1311
SMC	24.6861	37.5185	1.3234	2.0241

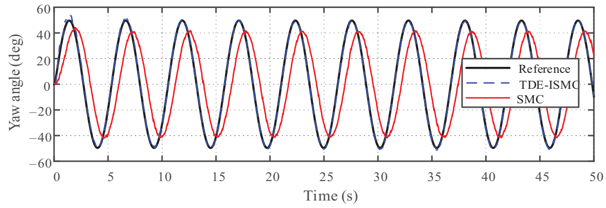

Figure 11. Tracking the performance of sine wave type (c) reference

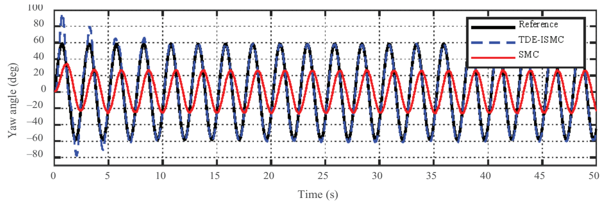

Figure 12. Tracking the performance of sine wave type (d) reference

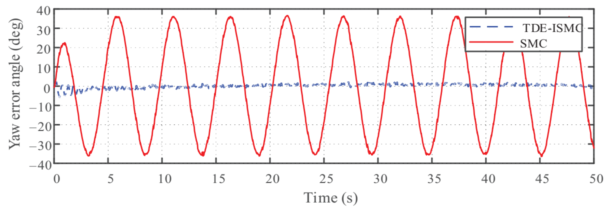

Figure 13. Error of tracking the performance of sine wave type (c) reference

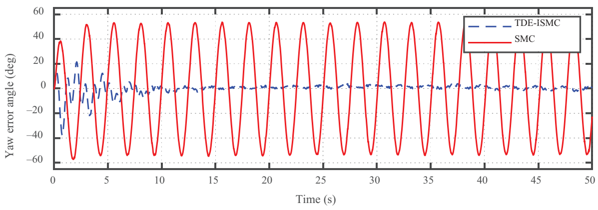

Figure 14. Error of tracking the performance of sine wave type (d) reference

The RMSE and ITAE values are also noted in Table 2, which shows the evaluation of both controllers. The SMC's values describe the instability of the whole system, while the high achievement is continuously in the proposed controller TDE-ISMC.

5. Conclusion

In this paper, the proposed controller TDE-ISMC is studied and conducted in the physical parameters of the single ducted-fan UAV. The stability of the whole physical system is guaranteed by the Lyapunov theory.

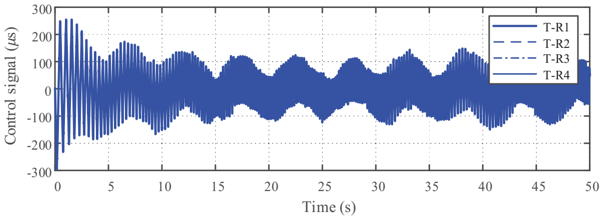

Figure 15. Control signal input of four actuators of TDE-ISMC (type c)

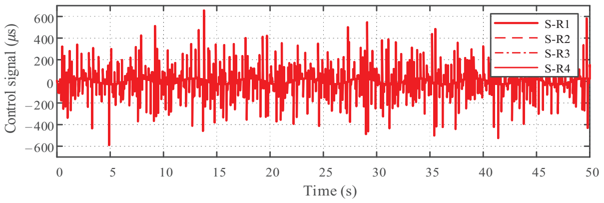

Figure 16. Control signal input of four actuators of SMC (type c)

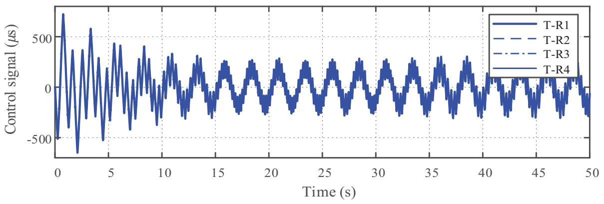

Figure 17. Control signal input of four actuators of TDE-ISMC (type d)

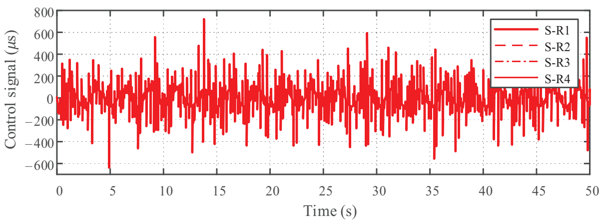

Figure 18. Control signal input of four actuators of SMC (type d)

The control law TDE-ISMC tackles the problem of the physical parameters, which is a complex system, and the incorrect identification of the parameters of DUAV.

For effectiveness and transparency, the simulation of both TDE-ISMC and classical SMC is conducted in four types of references. The proposed controller TDE-ISMC has a good performance in all types of references, while the classical SMC tracks poorly in the trapezium waves (scenario #1) and is unstable in the sine wave (scenario #2). To enhance the simulated results, the RSME and IEAT values of TDE-ISMC are better than the classical SMC. Therefore, the proposed method of control (TDE-ISMC) can work well to cope with the problems of the DUAV system, compared to classical SMC.

AUTHOR

Thien Minh Tran* – ORCID: 0000-0003-3465-5905, Department of Mechatronics, Faculty of Mechanical Engineering, HCMC University of Technology and Education (HCMUTE), Ho Chi Minh City, 700000, Vietnam, e-mail: thientm@hcmute.edu.vn.

*Corresponding author

ACKNOWLEDGEMENTS

This research received no external funding.

References

[1] K. Siciliano Khatib, *Handbook of Robotics*. Springer, 2016.

[2] A. Akturk and C. Camci, "Tip Clearance Investigation of a Ducted Fan Used in VTOL Unmanned Aerial Vehicles—Part I: Baseline Experiments and Computational Validation", *ASME Journal of Turbomachinery*, vol. 136, no. 021004, 2014, pp. 1–10.

[3] S. Sheng and C. Sun, "A Near-Hover Adaptive Attitude Control Strategy of a Ducted Fan Micro Aerial Vehicle with Actuator Dynamics", *Applied Sciences*, vol. 2015, no. 5, 2015, pp. 666–681. DOI: 10.3390/app5040666.

[4] M. V. Cook, *Flight Dynamics Principles*, Second edition, Elsevier, 2007.

[5] W. Fan, C. Xiang, and B. Xu, "Modelling, Attitude Controller Design and Flight Experiments of a Novel Micro-Ducted-Fan Aircraft", *Advances in Mechanical Engineering*, vol. 10, no. 3, 2018, pp. 1–16. DOI: 10.1177/1687814018765569.

[6] R. Naldi, L. Gentili, L. Marconi, and A. Sala, "Design and Experimental Validation of a Nonlinear Control Law for a Ducted-fan Miniature Aerial Vehicle", *Control Engineering Practice*, vol. 2010, no. 18, 2010, pp. 747–760. DOI: 10.1016/j.conengprac.2010.02.007.

[7] M.-T. Tran, D. H. Lee, S. Chakir, and Y.-B. Kim, "A Novel Adaptive Super-Twisting Sliding Mode Control Scheme with Time-Delay Estimation for a Single Ducted-Fan Unmanned Aerial Vehicle", *Actuators*, vol. 10, no. 54, 2021, pp. 1–28. DOI: 10.3390/act10030054.

[8] H. M. Abdelwaheb, K. Abderrahmane, and B. Aek, "Model-Free Sliding Mode Control for a Nonlinear Teleoperation System with Actuator Dynamics", *Journal of Automation, Mobile Robotics and Intelligent Systems*, vol. 14, no. 1, 2023, pp. 69–77. DOI: 10.14313/JAMRIS/1-2023/9.

[9] P. C. Sekhar and S. Mishra, "Sliding Mode Based Feedback Linearizing Controller for Grid Connected Multiple Fuel Cells Scenario", *Electrical Power and Energy Systems*, vol. 2014, no. 60, 2014, DOI: 10.1016/j.ijepes.2014.02.007.

[10] C. Edwards and S. K. Spurgeon, *Sliding Mode Control: Theory And Applications*. Taylor & Francis, 1998.

[11] M.-D. Hua, T. Hamel, P. Morin, and C. Samson, "Introduction to Feedback Control of Underactuated VTOL Vehicles", *IEEE Control Systems Magazine*, vol. 2013, 2013, pp. 61–75. DOI: 10.1109/MCS.2012.2225931.

[12] M.-T. Tran, T. Huynh, S. Chakir, D.-H. Lee, and Y.-B. Kim, "Angular Motion Control Design for a Single Ducted-Fan UAV using Robust Adaptive Pole-Placement Scheme in Presence of Bounded Disturbances", *Journal of Mechanical Science and Technology* vol. 36, no. 4, 2022, pp. 1–11. DOI: 10.1007/s12206-022-0338-9.

[13] A. Mazur and M. Kaczmarek, "Adaptive and Robust Following of 3D Paths by a Holonomic Manipulator", *Journal of Automation, Mobile Robotics and Intelligent Systems*, vol. 17, no. 3, 2023, pp. 65–77. DOI: 10.14313/JAMRIS/3-2023/23.

[14] K. J. Astrom and B. Wittenmark, *Adaptive control*. Dover Publications, 1994.

[15] M. S. Abdelkrim Brahmi, B. Brahmi, I. El Bojairami, G. Gauthier, and J. Ghommam, "Robust Adaptive Tracking Control for Uncertain Nonholonomic Mobile Manipulator", *Journal of Systems and Control Engineering*, vol. 2021, 2021, p. 11. DOI: 10.1177/09596518211027716.

[16] A. Nasry, A. Ezzahout, and F. Omary, "People Tracking in Video Surveillance Systems Based on Artificial Intelligence", *Journal of Automation, Mobile Robotics and Intelligent Systems*, vol. 17, no. 1, 2023, pp. 59–68. DOI: 10.14313/JAMRIS/1-2023/8.

[17] Y. Pan, C. Yang, L. Pan, and H. Yu, "Integral Sliding Mode Control: Performance, Modification and Improvement", *IEEE Transactions On Industrial Informatics*, 2018, DOI: 10.1109/TII.2017.2761389.

[18] J. Lee, P. H. Chang, and M. Jin, "Adaptive Integral Sliding Mode Control With Time-Delay Estimation for Robot Manipulators", *IEEE Transactions on Industrial Electronics*, vol. 64, no. 8, 2017, pp. 6796–6804. DOI: 10.1109/TIE.2017.2698416.

[19] J. Baek, M. Jin, and S. Han, "A New Adaptive Sliding-Mode Control Scheme for Application to Robot Manipulators", *IEEE Transactions On Industrial Electronics*, vol. 63, no. 6, 2016, pp. 3628–3637. DOI: 10.1109/TIE.2016.2522386.

[20] M. Jin, S. H. Kang, P. H. Chang, and J. Lee, "Robust Control of Robot Manipulators Using Inclusive and Enhanced Time Delay Control", *IEEE/ASME Transactions on Mechatronics*, vol. 22, no. 5, 2017, pp. 2141–2152. DOI: 10.1109/TMECH.2017.2718108.

[21] J. J. E. Slotine and W. Li, *Applied Nonlinear Control*. Prentice Hall, 1991.